Unidentified transitions in one-photon intrashell dynamics in Rydberg atoms

J. Preclíková,[1,*] A. Waheed,[1,2] D. Fregenal,[3] Ø. Frette,[1] B. Hamre,[1] B. T. Hjertaker,[1] E. Horsdal,[4] I. Pilskog,[1,5] and M. Førre[1]

[1]*Department of Physics and Technology, University of Bergen, N-5007 Bergen, Norway*
[2]*Higher Education Commission of Pakistan, Islamabad, Pakistan*
[3]*Centro Atómico Bariloche and Consejo Nacional de Investigaciones, Cientícas y Técnicas, R8402AGP S.C. de Bariloche, Argentina*
[4]*Department of Physics and Astronomy, Aarhus University, DK-8000 Aarhus C, Denmark*
[5]*Laboratoire de Chimie Physique Matière et Rayonnement, Université Pierre et Marie Curie - CNRS (UMR 7614),
75231 Paris Cedex 05, France*

One-photon intrashell transitions in strongly driven Li ($n = 25$) atoms are studied experimentally. The degeneracy of the n shell is lifted by orthogonal dc electric and magnetic fields, which also define the eccentricity of the initial coherent elliptic state. The transitions are driven by a radio frequency pulse linearly polarized parallel to the major axis of the ellipse. A small dc electric field component parallel to the magnetic field splits the one-photon resonance into two, and transitions in between are studied by state-selective field ionization. Unexpected lines in the ionization spectra relating to unknown transitions are found and discussed.

I. INTRODUCTION

Coherent elliptic states (CESs) are the quantum mechanical states most analogous to classical stationary states [1–8]. The electron density of a CES has an elliptic shape and is characterized by an eccentricity e that can be controlled by weak dc electric and magnetic fields. The quantum fluctuations of the defining, noncommuting angular momentum variables are as small as allowed by the uncertainty relations [1,6–8]. The formation of CESs in external fields was described in [2,3,8]. Intrashell dynamics of the Stark-Zeeman split $n = 25$ shell in Li was studied extensively over the last 10 years [9–17].

A CES of $e = 0$ is a circular spherical state of maximum l and m quantum numbers, $|n,l = n - 1,|m| = l\rangle$. Likewise, a CES of $e = 1$ is a Stark state of maximum polarization quantum number k [18], $|n,k = n - 1,m = 0\}$, a so called linear state. In alkali-metal Rydberg atoms, such linear states penetrate deeply into the core where the dynamical symmetry of the $1/r$ potential is broken. The elliptic states form a continuous set of states and the interaction with the core increases steadily when e is raised from 0 to 1.

Here we describe experimental studies of intrashell dynamics in Li ($n = 25$) atoms in a radio frequency (rf) field $\mathbf{E}_{rf}$. The atoms are initially prepared in a CES state of given eccentricity in the presence of perpendicular dc electric $\mathbf{E}_{dc}$ and magnetic $\mathbf{B}$ fields, and are then exposed to the linearly polarized pulse $\mathbf{E}_{rf}$. The major axis of the CES, $\mathbf{E}_{dc}$ and $\mathbf{E}_{rf}$ are parallel, and $\mathbf{B}$ is perpendicular to the orbital plane. $\mathbf{E}_{dc}$ and $\mathbf{B}$ lift the degeneracy of the n shell giving rise to one and multiphoton transitions when a multiple of the rf frequency is near resonance with the Stark-Zeeman splitting of the shell [17]. A small stray electric field parallel to $\mathbf{B}$ splits the one-photon resonance into two, and the dynamics in between is studied by state-selective field ionization (SFI) [18–20]. The stray field was remarkably stable over months. Unexpected, discrete lines were discovered and investigated systematically by varying the rf pulse duration and

intensity, n and e of the initial state, the Stark-Zeeman splitting of the shell, and the density of the cloud of Rydberg atoms.

Quantum calculations taking the lithium core into account within the framework of quantum defect theories [11,16,21] show that the dynamics in between the one-photon resonance is hydrogenic [16], that is, the nonhydrogenic core can be totally neglected, even when the atoms are strongly driven by the rf field. This stands in clear contrast to the situation at frequencies above, below, or at the two resonances where quantum defects are very important except when transitions are weakly driven. The calculated transition probabilities in between the resonances depend on the detailed pulse shape, but are generally small also at large rf field strengths. They cannot explain the strong, discrete lines seen here. Thus, the origin of these remains unknown.

II. EXPERIMENTAL ARRANGEMENT

The experimental arrangement was used earlier by Waheed *et al.* [17] who discussed it in detail. Here we repeat only what is important for the present discussion. A collimated thermal beam of lithium atoms is prepared in the vacuum chamber ($<10^{-6}$ mbar) by heating metallic lithium to $\approx$400 °C in an oven with a narrow exit channel. The thermal lithium atoms then pass through a Stark excitation region, an rf region, and finally pass into an SFI detection region.

In the Stark region, the atoms are resonantly excited by 3 ns laser pulses via the following transitions: $2s \rightarrow 2p \rightarrow 3d \rightarrow n = 25$. The required wavelengths 671, 610, and 831 nm are produced by three dye lasers pumped by 5 ns pulses of 532 nm light from a Nd:YAG laser operating at 14 Hz. A small thermal cloud of Rydberg atoms is thus formed at $t = 0$. Atoms of velocity $\simeq$2 mm/μs are subsequently selected.

The excitation occurs in the presence of a static electric field of 145 V/cm, which approximately gives the largest possible Stark splitting without significant inter-n mixing of the $n = 25$ shell. The wavelength of the laser that populates the $n = 25$ shell is tuned to excite the uppermost states of the Stark manifold. An even mixture of the three states $|nkm\} = |25,24,0\}$ and $|nkm\} = |25,23,\pm1\}$ is produced since the

*jana.preclikova@ift.uib.no

linewidth of the dye laser is 6 GHz and the energy gap between the neighboring states is about 3.4 GHz. A Fabry-Perot etalon was used in test runs to decrease the linewidth and selectively excite the two states. Identical behavior was found, so an even mixture was generally used to increase the signal to noise ratio.

When entering the rf region with the static fields, the atoms feel a gradual change of external conditions and adiabatically transform into CESs of eccentricity e given by [2,22]

$$e = \frac{\omega_S}{\omega_{SZ}}, \quad \text{where} \quad \omega_{SZ} = \sqrt{\omega_S^2 + \omega_L^2}, \quad (1)$$

and in atomic units

$$\omega_S = \frac{3}{2} n E_{dc} \quad \text{and} \quad \omega_L = \frac{B}{2}. \quad (2)$$

Here ω_S and ω_L are the Stark and Larmor frequencies, respectively, and ω_{SZ} is the Stark-Zeeman splitting of the shell. We used $\omega_{SZ}/2\pi = 95$ MHz, but checked that similar results are obtained with other choices.

At $t = 30 \, \mu$s, when the selected atoms are in the middle of the rf region, a linearly polarized rf pulse is applied. The rf pulse has a Gaussian-like envelope with a full width at half maximum (FWHM) that could be varied from 1 to 5 μs and a maximum within the range 0–1.2 V/cm [17].

The Rydberg atoms subsequently move into the SFI detection region. While moving into and properly inside this region they are stabilized by the magnetic field **B** (present in all three regions). The Rydberg atoms are finally detected by the SFI. For this purpose, a linear voltage ramp [23] was applied at $t = 60 \, \mu$s. It creates an electric ramping field $\mathbf{E}_{SFI}$ perpendicular to **B**, with a slew rate of $E_{SFI} \simeq 500 \, \text{V/cm} \, \mu\text{s}^{-1}$. $\mathbf{E}_{SFI}$ selectively ionizes different Rydberg states at different instants of time and accelerates the resulting Li$^+$ ions onto a channeltron detector operating in proportional mode. The signal is registered by a digital oscilloscope. The Stark, rf, and SFI regions are cooled to liquid nitrogen temperature in order to minimize the effect of blackbody radiation (BBR).

Although our chamber is made from stainless steel, every opening is covered by a copper mesh and plates are coated by antistatic graphite, a small unintended stray electric field $\mathbf{E}_s$ is present. The origin of this field is charged layers of deposits from the hot oven and/or contact potentials. For the dynamics of interest here, only the component of $\mathbf{E}_s$ parallel to **B** is important. It causes a symmetric splitting of the resonances relative to the unperturbed position [17]. From observed splittings 4 ± 1 MHz the field is estimated to be 40 ± 10 mV/cm.

III. RESULTS AND DISCUSSION

The SFI spectra in Fig. 1 depict typical outcomes of the experiment near the one-photon resonance. The uppermost spectrum represents the adiabatic spectrum of the 25 CES. The sharp onset at $t = 0 \, \mu$s is due to the prompt arrival of free ions into the detector after the ramp starts. These ions may result from multiphoton and collision processes. The broad background signal, which has a prolonged tail to longer times ($>3 \, \mu$s), is caused by radiative decay processes and the interaction with BBR [3,11].

BBR is also responsible for the multiple lines in the SFI spectra for CESs. The exposure from the excitation to the
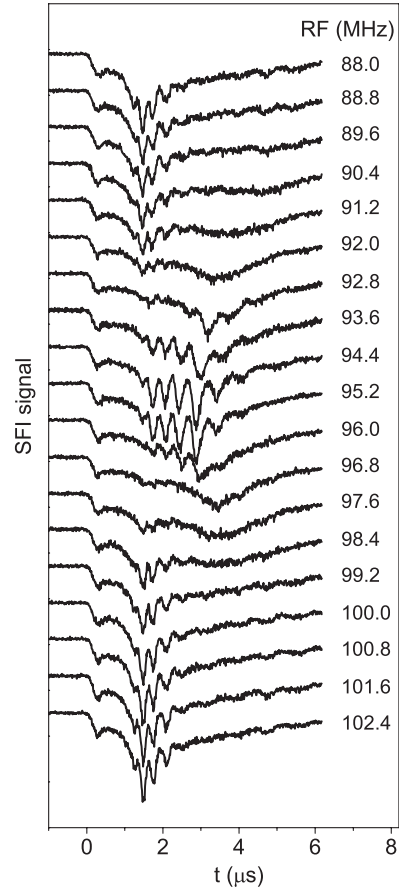

FIG. 1. SFI signals of Li Rydberg atoms. Initial circular states after interaction with rf pulses of frequencies from 88.0 to 102.4 MHz ($n = 25$, $\omega_{SZ}/2\pi = 95$ MHz, $E_{rf} = 0.44$ V/cm, and FWHM = 2.95 μs). Time measured from beginning of prompt signal of free ions.

turn-on of the rf pulse is about half of the total exposure to BBR. The Rydberg target in the rf region is thus more pure than indicated by the SFI spectra. Still, about 50% of the Rydberg atoms are in other states than the initial. The interaction with the BBR obeys dipole selection rules and connects circular CESs of different n. This seems to apply also for CESs of other e. Oscillator strengths are generally much weaker for s states than for CESs, see Fig. 2. This explains the qualitative difference between SFI spectra for the two types of states. The interaction with the BBR in the current setup was discussed in detail in Ref. [17].

The SFI spectra are completely different for atoms that do or do not interact with the rf pulse, see Fig. 1. The upper- and lowermost spectra at $f = 88.0$ and 102.4 MHz are typical adiabatic SFI spectra representing no interaction. The spectra near $f = 92.8$ and 96.8 MHz are typical diabatic SFI spectra representing strong interaction. For further details on adiabatic and diabatic SFI spectra see Refs. [11,14,17,18]. Finally, the two spectra at $f = 94.4$ and 95.2 MHz clearly show the unexpected line structure, the prime object of this study.

In the rest of this paper we focus on these structures. They occur at times 1.7–3.5 μs, corresponding to atoms ionizing in the field interval 850–1750 V/cm. Within this interval
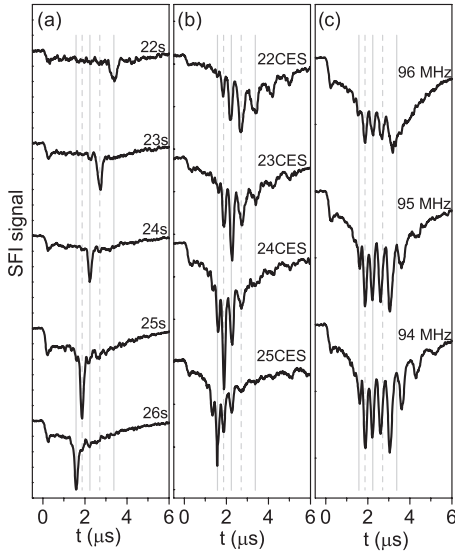
FIG. 2. SFI signals of Rydberg atoms excited to (a) ns states. (b) n CES of $e = 0.1$. No rf field. (c) 25 CES of $e = 0.1$ and three rf frequencies ($E_{rf} = 0.44$ V/cm, FWHM $= 2.95$ μs). Gray lines show ionization times of ns states.

they partly overlap with adiabatic lines on the lower side and diabatic continuous distributions on the upper.

A comparison with known SFI patterns is depicted in Fig. 2. In Fig. 2(a) $22s$–$26s$ SFI spectra are shown, while in Fig. 2(b) the corresponding CES spectra can be observed. We see that the most intense line of the n CES spectrum exactly overlaps the $(n + 1)s$ signal. This is because $\mathbf{E}_{SFI}$ shifts $(n + 1)s$ states down and n CESs up in energy. After the two states meet at $E_{SFI} \simeq 150$ V/cm the field takes them through a number of avoided crossings with each other until they ionize at the same field value (the classical limit). The lines of the unexplained structures shown in Fig. 2(c) do not overlap with the ns lines. Repeating the experiment with a different choice of shell splitting (46 MHz instead of 95 MHz) confirms these findings. This shows that the unexplained lines are probably not simply due to n CESs with $n < 25$.

In the next series of experiments we concentrated on mapping the conditions at which the new features are observed. Figure 3(a) depicts the evolution as a function of E_{rf}. From this, a threshold value of $\gtrsim 0.03$ V/cm is estimated under the given conditions. For larger fields no further evolution in character is observed. Variation of e, as shown in Fig. 3(b), reveals a gradual weakening of the line structure. Only a hint is left at $e = 0.5$.

We finally mention that extensive measurements at oven temperatures ranging from 345 to 678 °C only show marginal variation of the SFI line structure discussed here.

The weakening of the line structure with increasing eccentricity of the initial state can be attributed to the relative importance of the nonhydrogenic core. The modification of the system's wave function due to the Li core is in particular important for states containing a significant low-angular momentum component, which happens to be the case for states of high e. For instance, while an electron in a state with $e = 1$ penetrates deeply into the core region of the atom and probes the non-Coulombic part of the potential, an electron
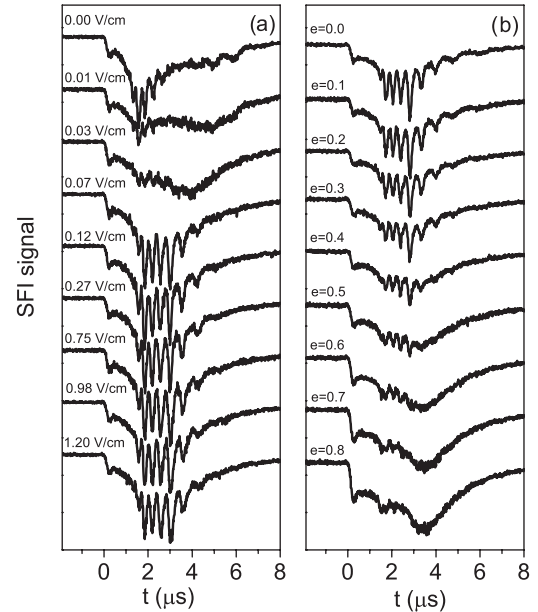

FIG. 3. SFI signals for 25 CES at shell splitting $\omega_{SZ}/2\pi = 95$ MHz. rf signal, $f = 95$ MHz and FWHM $= 2.95$ μs. (a) Various E_{rf} and $e = 0.1$. (b) Various e and $E_{rf} = 0.44$ V/cm.

in a circular state ($e = 0$) is far away from the core. This means that with increasing eccentricity of the initial state, the underlying dynamics becomes more and more nonhydrogenic. Our quantum calculations confirm this picture. Therefore, we anticipate that the gradual weakening of the line structure with increasing eccentricity [seen in Fig. 3(b)] is intimately related to a corresponding sliding breakdown of the hydrogenic approximation.

In our theoretical model for Li we have assumed the single-active-electron approximation where the outer Rydberg electron moves in a screened Coulomb potential set up by the core. The effect of the core is modeled within the framework of quantum defect theories (see Ref. [16] for further details about the theoretical model). Varying the value and direction of the stray field, applying pulses of different durations and intensity profiles, varying the strength of the rf field, and finally changing the eccentricity of the initial state, we could not find any explanation for the presence of the new structures in the SFI spectra. Even worse, starting out in a nearly circular initial state, theory actually predicts that nothing should happen at all, that is, according to theory the evolution of the system is fully adiabatic and the system's wave function eventually relaxes to the initial CES. This stands in clear contrast with the experimental data which clearly shows that transitions have occurred. As a matter of fact, we find this disagreement very surprising, as in our previous studies on intrashell dynamics in Li, the model was always capable of explaining the experimental results [11,13–16].

IV. CONCLUSION

In conclusion, we have investigated one-photon intrashell dynamics in lithium Rydberg shells that are Stark-Zeeman split in external dc fields. The splitting falls in the radio frequency regime. We report on evidence of new and unexpected spectral

features in the form of a characteristic line structure in the selective field ionization of the Rydberg atoms. This finding relates to transitions that we have not been able to identify. The line structure is seen only when the one-photon resonance is split by a small electric field parallel to the magnetic field contributing to the splitting of the shell, and only in between the two resulting resonances. The structure is remarkably stable toward variation of the rf field strength and duration, shell splitting, target density, and initial state (CES or states of similar shape). The structures disappear at large eccentricities ($e > 0.5$). Detailed quantum calculations [16,17] suggest that the dynamics is essentially hydrogenic between the resonances even for the largest rf field strengths considered here, and that the much simpler hydrogenic theory of Kazansky and Ostrovsky should apply [22]. Although the experimental results could be consistent with a scenario where population is transferred to higher m states (within the same n shell) that eventually field ionize diabatically, we have found no theoretical evidence for this. Therefore, we must conclude

that the modulations are due to transition channels not included in the theoretical model. Among such are two- or three-electron effects and harmonic generation in the individual Rydberg atoms, or collective effects in the gas of Rydberg atoms [24]. Blackbody radiation may be involved in this. The gas is quite special. Prior to the pulse of harmonic field it consists of Rydberg atoms in identical elliptic states all having the same orientation in space given by the angular momentum and Runge-Lenz vectors, which are controlled by external electric and magnetic fields.

[1] A. Bommier, D. Delande, and J.-C. Gay, in *Atoms in Strong Fields*, edited by C. A. Nicolaides *et al.* (Plenum, New York, 1990).

[2] J. C. Day, T. Ehrenreich, S. B. Hansen, E. Horsdal-Pedersen, K. S. Mogensen, and K. Taulbjerg, Phys. Rev. Lett. **72**, 1612 (1994).

[3] K. S. Mogensen, J. C. Day, T. Ehrenreich, E. H. Pedersen, and K. Taulbjerg, Phys. Rev. A **51**, 4038 (1995).

[4] R. G. Hulet and D. Kleppner, Phys. Rev. Lett. **51**, 1430 (1983).

[5] J. Liang, M. Gross, P. Goy, and S. Haroche, Phys. Rev. A **33**, 4437 (1986).

[6] J.-C. Gay, D. Delande, and A. Bommier, Phys. Rev. A **39**, 6587 (1989).

[7] C. Lena, D. Delande, and J. C. Gay, Europhys. Lett. **15**, 697 (1991).

[8] D. Delande and J. C. Gay, Europhys. Lett. **5**, 303 (1988).

[9] P. Sørensen, J. C. Day, B. D. DePaola, T. Ehrenreich, E. Horsdal-Pedersen, and L. Kristensen, J. Phys. B **32**, 1207 (1999).

[10] D. Fregenal, T. Ehrenreich, B. Henningsen, E. Horsdal-Pedersen, L. Nyvang, and V. N. Ostrovsky, Phys. Rev. Lett. **87**, 223001 (2001).

[11] M. Førre, D. Fregenal, J. C. Day, T. Ehrenreich, J. P. Hansen, B. Henningsen, E. Horsdal-Pedersen, L. Nyvang, O. E. Povlsen, K. Taulbjerg, and I. Vogelius, J. Phys. B **35**, 401 (2002).

[12] D. Fregenal, E. Horsdal-Pedersen, L. B. Madsen, M. Førre, J. P. Hansen, and V. N. Ostrovsky, Phys. Rev. A **69**, 031401(R) (2004).

[13] L. Nyvang, D. Fregenal, M. Førre, and E. Horsdal-Pedersen, J. Phys. B **37**, 4039 (2004).

[14] D. Fregenal, M. Førre, B. Henningsen, E. Horsdal, and D. Richards, Phys. Rev. A **76**, 053414 (2007).

[15] D. Fregenal, M. Førre, E. Horsdal, C. Fisker, and N. A Kjær, J. Phys. B **41**, 105003 (2008).

[16] I. Pilskog, D. Fregenal, Ø. Frette, M. Førre, E. Horsdal, and A. Waheed, Phys. Rev. A **83**, 043405 (2011).

[17] A. Waheed, D. Fregenal, O. Frette, M. Førre, B. T. Hjertaker, E. Horsdal, I. Pilskog, and J. Preclikova, Phys. Rev. A **83**, 063421 (2011).

[18] T. F. Gallagher, *Rydberg Atoms* (Cambridge University Press, New York, 1994).

[19] M. Førre and J. P. Hansen, Phys. Rev. A **67**, 053402 (2003).

[20] F. Robicheaux, C. Wesdorp, and L. D. Noordam, Phys. Rev. A **62**, 043404 (2000).

[21] M. Mijatović, E. A. Solov'ev, and K. Taulbjerg, J. Phys. B **34**, 1897 (2001).

[22] A. K. Kazansky and V. N. Ostrovsky, J. Phys. B **29**, L855 (1996).

[23] W. L. Fugua and K. B. MacAdam, Rev. Sci. Instrum. **56**, 385 (1985).

[24] R. H. Dicke, Phys. Rev. **93**, 99 (1954).